PROBABILITY OF FALSE ALARM ESTIMATION IN OVERSAMPLED ACTIVE SONAR SYSTEMS

Douglas A. Abraham

University of Connecticut
Electrical and Systems Engineering Dept., U-157
Storrs, CT 06269

phone: (860) 486-2192

email: d.a.abraham@ieee.org

ABSTRACT

The probability of false alarm (P_{fa}) in active sonar systems is an important system performance measure. This measure is typically estimated by the proportion of alarms to opportunities over some finite window, essentially forming the sample exceedance distribution function (EDF). It is common for sonar systems to be 'over-sampled'; that is, to have a sampling rate higher than the minimum required for representing the bandwidth of the received signal, resulting in reverberation data that are correlated from sample to sample. The performance of the sample EDF in P_{fa} estimation under such conditions is of interest. It is easily shown that the estimator remains unbiased with correlated data. However, it is shown in this paper that the variance of the estimator may be reduced from that for independent data by oversampling. Further, the variance is seen to fall between the Cramer-Rao lower bound based on independent thresholded (binary) data and that based on the complex matched filter output data.

1. INTRODUCTION

The probability of false alarm (P_{fa}) in active sonar systems is typically measured by counting the number of threshold exceedances (after normalization of the matched filter envelope or intensity data) within a finite window in time. Intuitively one would expect that this is best done with independent data samples. It will be shown in this paper that this is not necessarily so. Let the sequence $\ldots, X_i, X_{i+1}, \ldots$ be the normalized complex matched filter output of an active sonar system. If these data are reverberation-only samples and assuming ideal normalization, they would be zero-mean, unit-variance, complex Gaussian distributed (Rayleigh distributed envelope). Under these ideal assumptions and for some of the more straightforward normalization and detection algorithms, the P_{fa} of a detector is easily calculated and need not be estimated. However, there exist situations where it is necessary to estimate P_{fa} from real data, including complicated normalization and detection algorithms and sonar systems operating in ocean environments where the propagation and scattering conditions that result in reverberation do not produce a Rayleigh distributed envelope. The analysis in this paper assumes the ideal conditions under the premise that the results under non-ideal conditions are similar.

Depending on the sample rate of the system and the bandwidth of the transmit waveform, there may be substantial correlation between samples or very little. If the sample rate is near the bandwidth of the transmit waveform and the source and receiver characteristics and the propagation and scattering conditions result in complex Gaussian distributed reverberation with a nearly flat spectrum, the data should be (roughly) independent. It is, however, common for sonar systems to be oversampled and for these data to be used in estimating P_{fa}. If $Y_i = |X_i|^2$ are the intensity data and h is the detector threshold, then the sample exceedance distribution function (EDF) estimate of the P_{fa} will have the form

$$\hat{p} = \frac{1}{n}\sum_{i=1}^{n} U\left(Y_i - h\right) = \frac{1}{n}\sum_{i=1}^{n} Z_i \qquad (1)$$

where $U(y)$ is the unit step function and, for convenience, the n samples used in the estimate are numbered $i = 1, \ldots, n$. Clearly $Z_i = U\left(Y_i - h\right)$ is a Bernoulli random variable, taking on the value 1 with probability $p = \Pr\left\{Y_i > h\right\}$ and value 0 with probability $1 - p$. It is easily shown that $\hat{p}$ is unbiased ($\mathrm{E}\left[\hat{p}\right] = p$) without requiring independence of the samples. The following sections consider the variance of $\hat{p}$ for correlated data.

This work was performed while the author was with the SACLANT Undersea Research Centre, La Spezia, Italy

2. VARIANCE OF THE P_{FA} ESTIMATE

Assuming wide sense stationarity of the normalized reverberation data, the variance of $\hat{p}$ can be described as

$$\begin{aligned}\sigma_{\hat{p}}^2 &= \frac{1}{n^2}\sum_{i=1}^{n}\sum_{j=1}^{n}\mathrm{E}\left[(Z_i-p)(Z_j-p)\right] \\ &= \frac{p(1-p)}{n}\left[1+\frac{2}{n}\sum_{i=1}^{n-1}(n-i)\frac{r_i}{r_0}\right] \quad (2)\end{aligned}$$

where $r_i = \mathrm{E}\left[(Z_k-p)(Z_{k+i}-p)\right]$ for $i = 0,\ldots,n-1$. When the data are independent, $r_i = 0$ for $i = 1,\ldots,n-1$ and the variance is, as expected, $\frac{p(1-p)}{n}$.

In order to evaluate the sum of eq. (2), r_i must be obtained as a function of the spectrum of the complex matched filter output data. Towards this end, r_i can be related to the probability of the exceedance of both Y_k and Y_{k+i} over h,

$$\begin{aligned}r_i &= \mathrm{E}\left[Z_k Z_{k+i}\right] - p^2 \\ &= \mathrm{E}\left[U(Y_k-h)\,U(Y_{k+i}-h)\right] - p^2 \\ &= \Pr\{Y_k > h \text{ and } Y_{k+i} > h\} - p^2. \quad (3)\end{aligned}$$

Evaluation of eq. (3) requires integration over the joint probability distribution function (PDF) of Y_k and Y_{k+i} when the two samples are not independent. As shown in the Appendix, if the correlation between two of the complex matched filter output samples is $\gamma = \mathrm{E}\left[X_i X_j^*\right]$, then the joint PDF of their intensity values is

$$f(y_i, y_j; \gamma) = \frac{1}{1-|\gamma|^2}\mathrm{e}^{-\frac{y_i+y_j}{1-|\gamma|^2}} I_0\left(\frac{2|\gamma|\sqrt{y_i y_j}}{1-|\gamma|^2}\right), \quad (4)$$

where $I_0(x)$ is the zero$^{\text{th}}$ order modified Bessel function. After some manipulation it can be shown that r_i becomes

$$r_i = \int_{y=h}^{\infty} \mathrm{e}^{-y}\mathrm{E}\left(\frac{2h}{1-|\gamma_i|^2}; \frac{2y|\gamma_i|^2}{1-|\gamma_i|^2}\right) dy - p^2 \quad (5)$$

where $\gamma_i = \mathrm{E}\left[X_k X_{k+i}^*\right]$ and

$$\mathrm{E}(h;\delta) = \int_{x=h}^{\infty} \frac{1}{2}\mathrm{e}^{-\frac{(x+\delta)}{2}} I_0\left(\sqrt{\delta x}\right) dx \quad (6)$$

is the EDF for a non-central chi-squared random variable with two degrees of freedom and non-centrality parameter δ. Evaluation of eq. (5) may be accomplished numerically, exploiting the three-moment approximation to $\mathrm{E}(h;\delta)$ described in [1].

In order to evaluate eq. (2), the values of the autocorrelation function of the complex matched filter output for lags $m = 1,\ldots,n-1$ are used in eq. (5) to form the values $r_1,\ldots,r_{n-1}$. Assuming a flat reverberation spectrum when the sampling rate is equivalent to the transmit signal bandwidth, the oversampled spectrum would have the form of an ideal low-pass filter, resulting in the autocorrelation function

$$\gamma_D[m] = \frac{\sin\left(\frac{\pi m}{D}\right)}{\frac{\pi m}{D}} = \mathrm{sinc}\left(\frac{m}{D}\right) \quad (7)$$

where D is the oversampling factor (i.e., $D = 1$ results in independent data). If the reverberation data are well-represented by an AR process with spectrum

$$\Gamma(\omega) = \frac{c_0}{\left|1+\sum_{i=1}^{k} a_i \mathrm{e}^{-j\omega i}\right|^2} \quad (8)$$

when the sampling rate equals the bandwidth of the transmitted waveform, then the autocorrelation function of oversampled data is

$$\gamma_D[m] = c_0 \sum_{i=1}^{k} b_i p_i^{\frac{m}{D}} \quad (9)$$

where

$$b_i = c_i \sum_{l=1}^{k} \frac{c_l^*}{1-p_i p_l^*} \quad (10)$$

and (c_i, p_i) are respectively the residues and poles of

$$X(z) = \left(1+\sum_{i=1}^{k} a_i z^{-i}\right)^{-1}. \quad (11)$$

3. CRAMER-RAO LOWER BOUNDS

It is straightforward to show that the Cramer-Rao lower bound (CRLB) for p based on the data $\{Z_1,\ldots,Z_n\}$ is

$$\mathrm{CRLB}_Z = \frac{p(1-p)}{n}. \quad (12)$$

Note that the estimator of eq. (1) is efficient (i.e., its variance meets the CRLB) if only the binary data are available. As there is information lost in forming the binary data, the CRLB for the original complex data ($\{X_1,\ldots,X_n\}$) is also considered. Here it is assumed that the data have variance $\lambda = \frac{-h}{\log p}$, which results in the CRLB

$$\mathrm{CRLB}_X = \frac{(p\log p)^2}{n}. \quad (13)$$

It should be noted that the CRLB for the intensity data is identical to eq. (13). It is easily shown and intuitive that

$$\mathrm{CRLB}_X \leq \mathrm{CRLB}_Z \quad (14)$$

with equality only for $p = 1$.

4. ANALYSIS

To validate the theoretical analysis of the previous sections, the variance of the P_{fa} estimator is estimated from simulated and real data and compared with the theoretical values in Fig. 1, where good agreement is seen. In this example, $n = 500$ data samples were used (even after oversampling the data) to estimate the P_{fa}, with the threshold chosen so that $p = 0.01$. The real data were from a 125 Hz bandwidth LFM waveform and were tested to insure Gaussianity and an approximately flat spectrum. The analytical results assumed the autocorrelation function of eq. (7). As one would expect, the variance of the P_{fa} estimate increases with the oversampling factor because the effective number of independent samples decreases. However, the variance of $\hat{p}$ using the oversampled data is less than that of $\hat{p}$ just using the equivalent number of independent samples ($= \frac{n}{D}$). This is, perhaps, a non-intuitive result that requires some discussion. Sampling theory tells us that if a signal is sampled above the Nyquist rate, it (ideally) may be perfectly reconstructed. Oversampling is a step toward reconstruction, filling in what's missing between the independent samples and providing a more accurate picture of what's happening around the threshold. This apparently leads to a reduction in the variance of the P_{fa} estimator.

Next, consider the CRLBs of the previous section. Figure 2 shows n times the CRLBs and n times the variance of $\hat{p}$ as a function of p (effectively the CRLB and variance per sample). As opposed to the analysis associated with Fig. 1, $n_0 = 500$ independent data samples were always used here, so the oversampled cases used $n = n_0 D$ (correlated) samples. The CRLB for the binary data and the variance of the independent data ($D = 1$) are identical. However, oversampling reduces the variance and shifts the curve down toward the CRLB for the complex data. Oversampling by more than $D = 5$ did not provide significant improvement.

In Fig. 3, the ratio of the variance of $\hat{p}$ with oversampling to that for independent data,

$$\Delta(D, n_0) = \frac{\sigma^2_{\hat{p}}(D, n_0 D)}{\sigma^2_{\hat{p}}(1, n_0)}, \tag{15}$$

is shown for various P_{fa} values, where $\sigma^2_{\hat{p}}(D, n)$ is the variance of $\hat{p}$ using D times oversampling and n samples ($\frac{n}{D}$ independent samples). The reduction in variance increases with the oversampling factor, although the majority is obtained by the time $D = 4$. The results for this figure were obtained by using $n_0 = 500$. However, the results for $n_0 = 500$ and $n_0 = 1000$ were visually indistinguishable. It is not believed that $\Delta(D, n_0)$ is independent of n_0, but that it rapidly approaches an asymptotic value with n_0. This comment holds for the results shown in Fig. 2 and also under the AR process autocorrelation values of eq. (9).

5. CONCLUSIONS

The variance of the standard P_{fa} estimator was derived analytically for correlated data. The analysis leads to the interesting conclusion that oversampling the reverberation time series results in a reduction in the variance of the P_{fa} estimate. It was seen that the majority of the improvement is obtained by the time the data are oversampled by a factor of four, a result that seems to be independent of the size of the window used to estimate the P_{fa}, assuming some minimum size. The variance was compared with the CRLBs obtained from independent complex matched filter output data or independent binary thresholded data. Though not an efficient estimator compared with the complex matched filter output CRLB, oversampling was seen to provide improvement over that obtainable with binary independent data. The implications of this result on the false alarm and detection performance over a full ping of data, where the correlation introduced by oversampling makes analysis difficult, are unknown and worthy of further research.

6. REFERENCES

[1] N. L. Johnson, S. Kotz, and N. Balakrishnan, *Continuous Univariate Distributions*, vol. 2, John Wiley & Sons, Inc., second edition, 1995.

A. JOINT PDF OF CORRELATED INTENSITY DATA

If the pair (V, U) are unit-variance, zero-mean complex random variables with a correlation $\gamma = \mathrm{E}[VU^*]$, then their joint PDF has the form

$$f(v, u) = \frac{1}{\pi^2 \left(1 - |\gamma|^2\right)} \times \exp\left\{ \frac{-1}{1 - |\gamma|^2} \left[|v|^2 + |u|^2 - 2\Re(\gamma^* v^* u) \right] \right\}, \tag{16}$$

where $\Re(v)$ is the real part of v. Transformation to an intensity-angle parameterization results in

$$f(y, z, \theta, \phi) = \frac{1}{4\pi^2 \left(1 - |\gamma|^2\right)} \times \exp\left\{ \frac{-1}{1 - |\gamma|^2} \left[y + z + 2|\gamma| \sqrt{yz} \cos(\phi - \theta - \beta) \right] \right\} \tag{17}$$

where $v = \sqrt{y} e^{j\theta}$, $u = \sqrt{z} e^{j\phi}$, and $\gamma = |\gamma| e^{j\beta}$. Integration over both θ and ϕ from 0 to 2π then results in eq. (4).

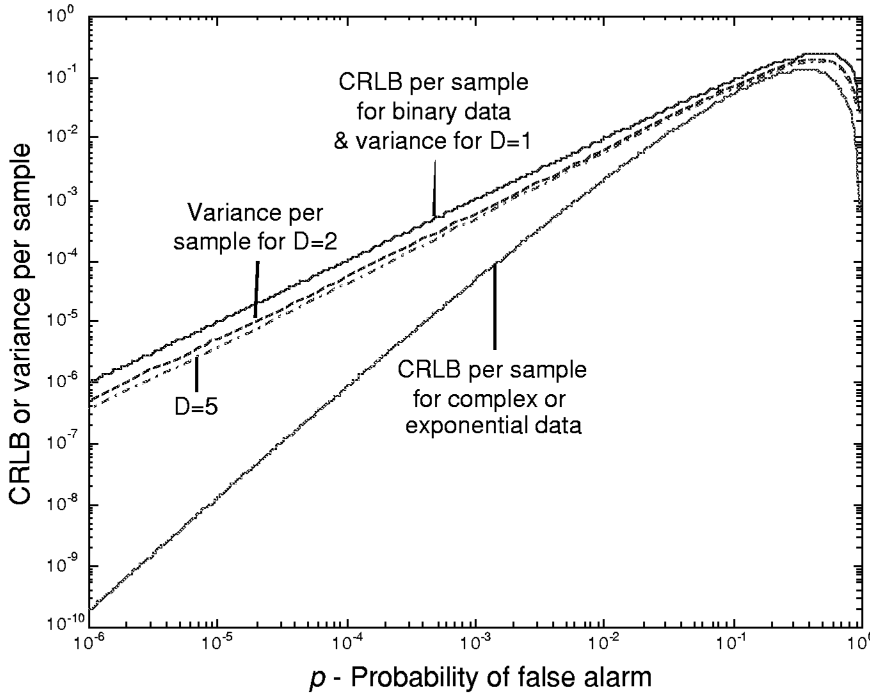

Figure 2: CRLBs and variance per sample as a function of P_{fa}.

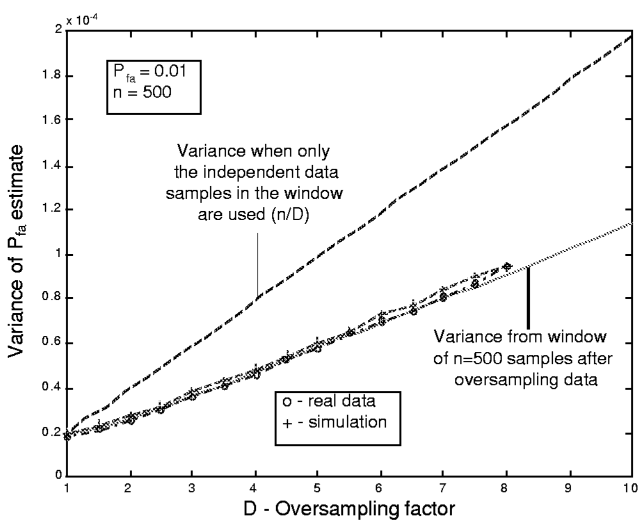

Figure 1: Variance as a function of oversampling, keeping n fixed at 500.

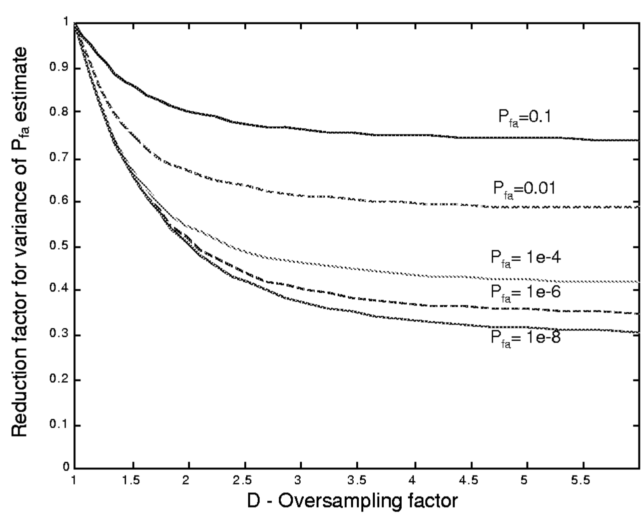

Figure 3: Reduction factor of variance as a function of oversampling.